Synthesis of Five-bar Motion Generation with Gear Train Fabrication Tolerances

S. Mutawe, NJIT, Newark, USA
R.S. Sodhi, NJIT, Newark, USA
Y.M. Al-Smadi*, AECOM, New York, USA
A. Bhargava, AECOM, New York, USA
M. Mahgoub, NJIT, Newark, USA

Abstract— *Geared Five-bar motion generation is used to synthesize a mechanism which passes through or approximate prescribed rigid-body positions. This work will discuss the motion generation of geared five-bar mechanism with position tolerance variations due to gear fabrication. The tolerance variations study will be based on the standards of American Gear Manufacturing Association (AGMA) and American National Standard Institute (ANSI). The new design constraint introduced in this paper will consider the gear train tolerances and incorporate it into the displacement position matrix of coupler points described in the conventional planar five-bar motion generation models developed by [1] and [2]. The synthesized planar geared five-bar mechanism will produce tolerance limits for moving pivots and link length from which any mechanism can be synthesized to satisfy the prescribed coupler points with their prescribed tolerances. The included example demonstrates the synthesis of a geared five-bar mechanism with gear train tolerances.* [1]

Keywords: Motion Generation, Coupler points Tolerances, Geared Five-bar mechanism, Gear Tolerance,

I. Introduction

The objective of geared five-bar motion generation is to calculate the mechanism parameters required to achieve or approximate a set of prescribed rigid-body poses. This mechanism design objective is particularly useful when the rigid-body must achieve a specific displacement sequence for effective operation (e.g., specific tool paths and/or orientations for accurate fabrication operations). In Fig. 1 four prescribed rigid-body poses are defined by the coordinates of variables **p**, **q**, and **r** (motion generation model input), and the model outputs are the calculated coordinates of the moving pivot variables $\mathbf{a}_1$ and $\mathbf{c}_1$ and the scalar link lengths R_1 and R_3.

Planar mechanism synthesis with tolerances is a well-established field. These tolerances can be found in joints and linkages due to many factors such as manufacturing processes, loading and unloading of the mechanism which increases joint clearance after service period and causes impulsive forces. This paper investigates the tolerances caused by gear fabrication and their effect on the synthesis of geared five-bar mechanism. Several methods and analyses have been used to include the error caused by joint clearances and link geometry tolerances in the mechanism synthesis. Graphical and mathematical approaches to investigate the efficiency of planar mechanisms to approximate the coupler poses considering the errors/tolerances in mechanism linkages were developed by [3] and [4]. Recent contributions performed by [5, 6 and 7] modeled the joint clearance as a massless virtual link (clearance link) and investigated the joint clearance effect on the mechanism performance to achieve the prescribed coupler curves/points. A method to predict the limits of the tolerance region by choosing the clearance value was also proposed by [7].

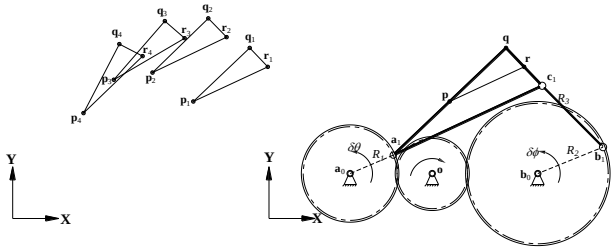

Fig. 1: Prescribed rigid-body poses and calculated planar five-bar mechanism

Mechanism performance to achieve the prescribed/desired positions can be affected by joint clearance and link dimension tolerances. This paper investigates the gear fabrication tolerances developed by ANSI/AGMA on the mechanism performance.

II. Conventional planar five-bar motion generation analysis

Equations (1) through (3) encompass a conventional planar five-bar motion generation model presented by [1]

$$\left([\mathbf{D}_{1j}]\mathbf{a}_1-\mathbf{a}_0\right)^T\left([\mathbf{D}_{1j}]\mathbf{a}_1-\mathbf{a}_0\right)-L_1^2=0\,, \tag{1}$$

$$\left([\mathbf{D}(\delta\varphi)_{1j}]\mathbf{b}_1-\mathbf{b}_0\right)^T\left([\mathbf{D}(\delta\varphi)_{1j}]\mathbf{b}_1-\mathbf{b}_0\right)-L_2^2=0\,, \tag{2}$$

$$\left([\mathbf{D}_{1j}]\mathbf{c}_1-[\mathbf{D}(\delta\varphi)_{1j}]\mathbf{b}_1\right)^T\left([\mathbf{D}_{1j}]\mathbf{c}_1-[\mathbf{D}(\delta\varphi)_{1j}]\mathbf{b}_1\right)-L_3^2=0 \tag{3}$$

where j=1,2,3,4

* Yahia.Al-Smadi@aecom.com
13th World Congress in Mechanism and Machine Science, Guanajuato, México, 19-25 June, 2011

These equations are "constant length" constraints and ensure the fixed length of links $\mathbf{a}_0$-$\mathbf{a}_1$, $\mathbf{b}_0$-$\mathbf{b}_1$, and $\mathbf{b}_1$-$\mathbf{c}_1$ throughout the prescribed rigid-body displacements. Variables L_1, L_2, and L_3 in Equations (1) through (3) are the prescribed scalar lengths of links $\mathbf{a}_0$-$\mathbf{a}_1$, $\mathbf{b}_0$-$\mathbf{b}_1$, and $\mathbf{b}_1$-$\mathbf{c}_1$ respectively.

$$\left[\mathbf{D}_{1j}\right]=\begin{bmatrix} p_{jx} & q_{jx} & r_{jx} \\ p_{jy} & q_{jy} & r_{jy} \\ 1 & 1 & 1 \end{bmatrix}\begin{bmatrix} p_{1x} & q_{1x} & r_{1x} \\ p_{1y} & q_{1y} & r_{1y} \\ 1 & 1 & 1 \end{bmatrix}^{-1}, \tag{4}$$

$$\left[\mathbf{D}(\delta\varphi)_{1j}\right]=\begin{bmatrix} \cos(\delta\varphi)_{1j} & -\sin(\delta\varphi)_{1j} & -b_{0x}\cos(\delta\phi)_{1j}+b_{0y}\sin(\delta\phi)_{1j}+b_{0x} \\ \sin(\delta\varphi)_{1j} & \cos(\delta\varphi)_{1j} & -b_{0x}\sin(\delta\phi)_{1j}-b_{0y}\cos(\delta\phi)_{1j}+b_{0y} \\ 0 & 0 & 1 \end{bmatrix} \tag{5}$$

where j=1,2,3,4

Equation (4) is a rigid-body planar displacement matrix. Equation (5) is the angular displacement matrix for link $\mathbf{b}_0$-$\mathbf{b}_1$ where $(\delta\varphi)_{1j}=k(\delta\theta)_{1j}$. Variable k represents the gear ratio of the gear train joining grounded links $\mathbf{a}_0$-$\mathbf{a}_1$ and $\mathbf{b}_0$-$\mathbf{b}_1$. From this conventional planar five-bar motion generator model, 12 of the 13 unknown variables $\mathbf{a}_0$, $\mathbf{a}_1$ L_1, $\mathbf{b}_0$, $\mathbf{b}_1$, L_2, $\mathbf{c}_1$, and L_3 are calculated with one arbitrary choice of parameter (where $\mathbf{a}_0=[a_{0x}, a_{0y}, 1]$, $\mathbf{a}_1=[a_{1x}, a_{1y}, 1]$, $\mathbf{b}_0=[b_{0x}, b_{0y}, 1]$, $\mathbf{b}_1=[b_{1x}, b_{1y}, 1]$, and $\mathbf{c}_1=[c_{1x}, c_{1y}, 1]$).

III. Modeling of rigid-body poses Tolerance

This paper presents a technique of synthesizing planar geared five-bar mechanism considering gear train tolerances. Insensitive analyses for optimal coupler points trajectory have been performed in mechanism synthesis, many goal functions have been formulated in an effort to define the linkages with a tolerance to approximate the desired coupler points trajectory with tolerable accuracy. Investigations carried out by [20] and [21] on RRCC mechanism and multi-phase five-bar mechanism respectively show the mechanism motion synthesis with a prescribed tolerance for one position, while work presented in [8] shows analytical solutions for the kinematic analysis of position, velocity, acceleration and transmission angle of geared linkage mechanisms. Several optimization algorithms, objective/goal functions and techniques on the shape of coupler curve and points have been presented in [15-18]. Al-Smadi et al [12] developed a nonlinear optimization to investigate geared five-bar with structural constraints. This research adds the consideration of the calculated gear train tolerances to the synthesis of the geared five-bar mechanisms.

The tolerances selected for this study is in accordance with [13] which specifies many variations for gear fabrications, four main variations were selected and presented herein. For any prescribed rigid-body pose to be achieved, the plus or minus deviation from the specified value would be the allowable tolerance limits. The gear fabrication variations such as face width variation, spacing variation and many others affect the gear meshing, and consequently affect the accuracy of achieving the prescribed rigid-body poses for the geared five-bar mechanism. This paper will discuss four variations which are radial runout variation, pitch variation, profile variation, and tooth thickness variation.

IV. Gear Fabrication Tolerance Synthesis

In this paper, the gear train used to drive the planar five-bar mechanism consists of spur gear type only. Spur gear is subject, but not limited to the following tolerance:

Radial runout variation (V_{rT}) which is the runout of the teeth measured in a direction normal to the datum axis of rotation. The formula for this variation according to [13] is

$$\pm V_{rT} = 58.0(N)^{0.238}(P_{nd})^{-0.722}(1.4)^{(8-Q)} \tag{6}$$

where N= number of teeth, P_{nd} = diametral pitch and Q = Gear quality number.

Pitch Variation (V_{pA}) as shown in Fig. 2 which is the maximum allowable amount of the difference between the true position pitch and an actual pitch as described in Fig. 2. The formula for this variation according to [13] is

$$\pm V_{pA} = 10.5(N)^{0.177}(P_{nd})^{-0.401}(1.42)^{(8-Q)} \tag{7}$$

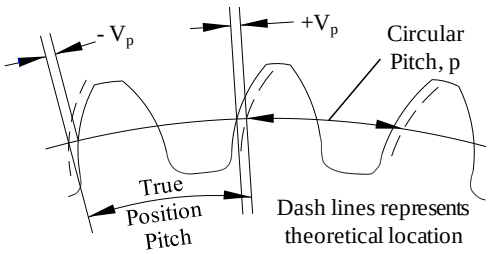

Fig. 2: Pitch Variation

Profile variation (V_{ϕ}) as shown in Fig. 3 which is the difference between the actual and the specified functional profile. The formula for this variation according to [13] is

$$\pm V_{\phi T} = 21.5(N)^{0.154}(P_{nd})^{-0.589}(1.4)^{(8-Q)} \tag{8}$$

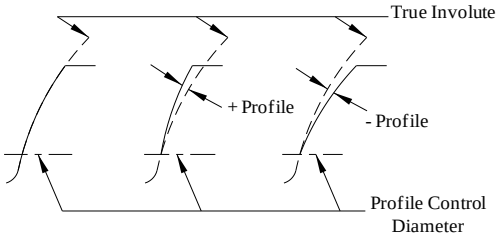

Fig. 3: Profile variations.

Tooth thickness tolerance (t_T) as shown in Fig. 4 which is the permissible amount of difference between actual and theoretical value of circular tooth thickness. The formula for this variation according to [13] is

$$\pm t_T = 0.03769(2)^{1-L_n}(P_{nd})^{-1} \quad (9)$$

where L_n = 1,2,3,4

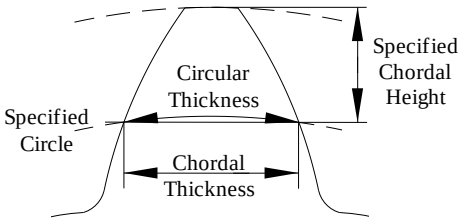

Fig. 4: Circular tooth thickness

The total gear train tolerance is the sum of equations 6 through 9.

$$\delta = V_{pA} + V_{rT} + V_{\phi T} + t_T \quad (10)$$

V. Modification of poses displacement matrix considering tolerance

Gear train inherent tolerance would affect and produce a tolerance region for each coupler point to be positioned within. Research performed by [14] and [15] presented that the region of the moving pivot point in four-bar mechanism takes the shape of a rectangle with curved sides. If δ_x and δ_y applied on each coupler point pose, then a tolerance region of a box shape would predict the limits with reasonable accuracy. [16, 17and 18] concluded that the tolerance region for coupler point positions is an ellipse shape. Using reliability analysis in mechanism synthesis, [19] formed a reliable region S_R for RCCC Mechanism. Russell and Sodhi [20] considered point tolerance for RRSS mechanism by considering δ_x and δ_y for one pose only. This consideration would produce a tolerance region of a box shape if covariance is not calculated; this consideration still produces a tolerance region with reasonable accuracy. Similar consideration was performed by [21] in which a square tolerance region for one coupler point pose was suggested. Design sensitivity of an elliptical tolerance region versus square shape tolerance region was formulated by [22]. The tolerance region presented in this paper is considered as a square or a box shape. The work of [7], [20] and [21] for choosing the clearance value has been adopted. Therefore, Equation 10 is defined to enumerate the maximum tolerance value formed for each coupler point pose 1 through 4. Figure 5 shows the tolerance regions limited by $\pm\delta_x$ and $\pm\delta_y$ for coupler points **p**, **q** and **r**.

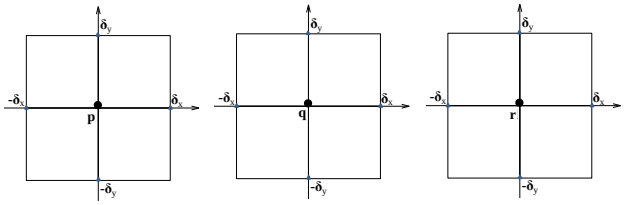

Fig. 5: Tolerance region

The tolerance calculated from Equation 10 will be used in the poses matrix of the coupler points $[\mathbf{D}_j]$ and the displacement matrix $[\mathbf{D}_{1j}]$ as shown in Equations 11 and 12. Several cases of tolerance limits (i.e. 0δ, $+\delta_x$, $-\delta_x$, $+\delta_y$, $-\delta_y$, $+\delta_x$ and $+\delta_y$, $-\delta_x$ and $-\delta_y$, $+\delta_x$ and $-\delta_y$, and $-\delta_x$ and $+\delta_y$) are investigated, moving pivots $\mathbf{a}_1$, $\mathbf{c}_1$ and Links R_1 and R_3 are synthesized for each case.

$$[\mathbf{D}_j] = \begin{bmatrix} p_{jx} \pm \delta_x & q_{jx} \pm \delta_x & r_{jx} \pm \delta_x \\ p_{jy} \pm \delta_y & q_{jy} \pm \delta_y & r_{jy} \pm \delta_y \\ 1 & 1 & 1 \end{bmatrix} \quad (11)$$

$$[\mathbf{D}_{1j}] = \begin{bmatrix} p_{jx} \pm \delta_x & q_{jx} \pm \delta_x & r_{jx} \pm \delta_x \\ p_{jy} \pm \delta_y & q_{jy} \pm \delta_y & r_{jy} \pm \delta_y \\ 1 & 1 & 1 \end{bmatrix} \begin{bmatrix} p_{1x} & q_{1x} & r_{1x} \\ p_{1y} & q_{1y} & r_{1y} \\ 1 & 1 & 1 \end{bmatrix}^{-1} \quad (12)$$

where j=2,3,4

VI. Example

Motion generation program can be used with prescribed values of $\mathbf{a}_0$=(0, 0), $\mathbf{b}_0$=(25, 0), $\mathbf{b}_1$=(33, 12), and R_2=10, and initial guesses of $\mathbf{a}_1$=(10, 5), R_1=10, $\mathbf{c}_1$=(20, 20), and R_3=15. Gear nomenclatures and the calculated value of tolerance (δ) are shown in Table 1. Gear train tolerance calculated in Table 1 will be used to generate the area described in Section V. Coupler poses can fall anywhere within that region. Therefore, nine tolerance cases has been discussed and investigated. The solutions of the achieved mechanism parameters (a_{1x}, a_{1y}, R_1, c_{1x}, c_{1y}, R_3) are shown in Table 2. Rigid-body poses 1 through 4 correspond to link $\mathbf{a}_0$-$\mathbf{a}_1$ rotation angles of θ_1= 75°, 89.4°, 111°, and 125.4° respectively. Therefore the displacement angles $(\delta\theta)_{1j}$ for link $\mathbf{a}_0$-$\mathbf{a}_1$ are 14.4°, 36° and 50.4° respectively. The angle displacements $(\delta\varphi)_{1j}$ for link $\mathbf{b}_0$-$\mathbf{b}_1$ corresponds to $(\delta\varphi)_{1j}=k(\delta\theta)_{1j}$, where k represents the gear ratio which is equal to 0.5, the angle displacements $(\delta\varphi)_{1j}$ for link $\mathbf{b}_0$-$\mathbf{b}_1$ corresponds to 7.2°, 18° and 25.2° respectively.

Nomenclature	Gear 1	Gear 2	Gear 3
Pitch Diameter (D)	5	5	10
Number of Teeth (N)	10	10	20
Diametral Pitch (P_{nd})	2	2	2
Gear Quality (Q)	4	4	4
Gear Class (L_n)	1	1	1
Tolerance			
Pitch (V_{pA}) =	±0.0048	±0.0048	±0.0055
Radial Runout (V_{rT})=	±0.0234	±0.0234	±0.0276
Profile ($V_{\varphi T}$) =	±0.0078	±0.0078	±0.0087
Tooth Thickness (t_T)=	±0.0188	±0.0188	±0.0188
Gear Tolerance (δ) =	±0.0548	±0.0548	±0.0606
Gear Train Tolerance = ($\delta_{Gear\ 1}$+ $\delta_{Gear\ 2}$+ $\delta_{Gear\ 3}$)	±0.1702		

TABLE1. Gear Nomenclature and Tolerances

	0δ	$+\delta_x$	$-\delta_x$	$+\delta_y$	$-\delta_y$	$+\delta_x$,$+\delta_y$	$-\delta_x$,δ_y	$+\delta_x$,$-\delta_y$	$-\delta_x$,δ_y
a_{1x}	2.070	2.067	2.072	2.074	2.066	1.902	2.230	2.063	2.077
a_{1y}	7.727	7.694	7.761	7.684	7.771	7.841	7.97	7.738	7.717
R_1	8.000	7.967	8.033	7.956	8.044	7.924	8.07	8.010	7.990
c_{1x}	20.30	20.87	19.66	22.14	17.82	22.37	17.0	18.65	21.69
c_{1y}	19.75	19.47	20.06	18.88	20.91	18.52	21.5	20.52	19.10
R_3	14.98	14.35	15.70	12.95	17.72	12.50	18.8	16.80	13.45

TABLE 2. Calculated coordinates of the moving pivot variables $\mathbf{a_1}$ and $\mathbf{c_1}$ and scalar link lengths R_1 and R_3 for nine combination cases of tolerance δ

Synthesized mechanisms which consist of the achieved moving pivot points $\mathbf{a}_1$ and $\mathbf{c}_1$ and link lengths R_1 and R_3 shown in Table 2 and prescribed values of $\mathbf{a}_0$, $\mathbf{b}_0$, $\mathbf{b}_1$ and link R_2 were constructed. All rigid-body poses achieved by the constructed mechanisms were investigated. They were found to be comparable with the prescribed poses and were within the calculated gear train tolerance range. Two examples (highlighted cases shown in Table 2) are presented from this investigation, others can be done similarly. Case 1 represents precise rigid-body poses (i.e. δ=0) and Case 6 when $+\delta_x$ and $+\delta_y$ are considered, this case produces the shortest link lengths R_1 and R_3. Table 3 includes the x and y-coordinates (in inches) of four prescribed rigid-body poses with zero tolerance, for coupler points p, q and r. Table 4 includes the rigid-body poses calculated after incorporating the parameters of the synthesized mechanism for case 1. Tables 5 and 6 include the prescribed and achieved poses respectively for the tolerance case of $+\delta_x$ and $+\delta_y$.

	P	**q**	**r**
Pose 1	20.4523, 32.0987	37.3158, 38.7974	32.3130, 28.8679
Pose 2	18.4699, 32.3675	35.3346, 39.0632	30.3300, 29.1346
Pose 3	15.0774, 32.1637	31.8188, 39.1621	26.9938, 29.1450
Pose 4	12.5850, 31.7271	29.1160, 39.2089	24.5841, 29.0558

TABLE 3. Prescribed rigid-body poses for δ=0

	p	**q**	**r**
Pose 1	20.4523, 32.0987	37.3158, 38.7974	32.3130, 28.8679
Pose 2	18.4698, 32.3675	35.3345, 39.0632	30.3299, 29.1346
Pose 3	15.0773, 32.1636	31.8188, 39.1617	26.9937, 29.1446
Pose 4	12.5850, 31.7268	29.1161, 39.2083	24.5840, 29.0553

TABLE 4. Rigid-body poses achieved by synthesized planar five-bar mechanism for δ=0

	p	**q**	**r**
Pose 1	20.4523, 32.0987	37.3158, 38.7974	32.3130, 28.8679
Pose 2	18.6402, 32.5378	35.5049, 39.2335	30.5003, 29.3049
Pose 3	15.2477, 32.3340	31.9891, 39.3324	27.1641, 29.3153
Pose 4	12.7553, 31.8974	29.2863, 39.3792	24.7544, 29.2261

TABLE 5. Prescribed rigid-body poses for δ_x= δ_y =+0.1702

	p	**q**	**r**
Pose 1	20.4523, 32.0987	37.3158, 38.7974	32.3130, 28.8679
Pose 2	18.4620, 32.4160	35.3055, 39.1647	30.3322, 29.2204
Pose 3	15.0700, 32.3000	31.7619, 39.4156	27.0073, 29.3649
Pose 4	12.5746, 31.9289	29.0367, 39.5610	24.5975, 29.3670

TABLE 6. Rigid-body poses achieved by synthesized planar five-bar mechanism for δ_x= δ_y =+0.1702

The ranges of the achieved pivot variables for the given tolerance region are represented by the perimeter of the solid line in the plots of Fig. 6. The perimeter represents the value of these pivot variables for which, the rigid-body position tolerances will be within the prescribed limit. For the given tolerance, a least square best fit can be obtained for each of the variables. These best fit curves are represented in Fig. 6 using dashed-line format. Since only nine cases were analyzed here, the shape of the best fit curve is a nine-sided polynomial.

But, a close examination of the data clearly indicates that for the entire square tolerance region (Fig. 5) the best fit curve will be a circle. The radius of this best fit curve represents the values of the pivot variable for which the given tolerances will always be met.

To examine the best-fit curve tolerance, pivot points $\mathbf{a_1}$ and $\mathbf{c_1}$ and link lengths R_1 and R_3 were selected such that the difference between the solid and dashed lines is maximum, this selection corresponds to the case of considering both -δx and -δy (Fig. 6). The selected moving pivot coordinates and mechanism crank and follower lengths of the geared five-bar motion (Fig. 7) generator are $\mathbf{a_1}$=(2.0734, 7.7903), $\mathbf{c_1}$=(20.4741, 1.4970), 7.9905 inch and 14.7859inch respectively. Using ADAMS module in Solidworks, the achieved coupler poses in Table 7 were measured for the geared five-bar motion generator (Fig. 7). Table 8 includes the scalar differences ($\left|point_{prescibed} - point_{achieved}\right|$) between the prescribed (Table 3) and achieved (Table 7) coupler poses of the synthesized motion generator.

	p	q	r
Pose 1	20.4523, 32.0987	37.3158, 38.7974	32.3130, 28.8679
Pose 2	18.4919, 32.3492	35.3625, 39.0300	30.3492, 29.1058
Pose 3	15.1071, 32.1209	31.8627, 39.0848	27.0173, 29.0776
Pose 4	12.6204, 31.6673	29.1715, 39.1045	24.6122, 28.9637

TABLE 7. Rigid-body poses achieved by synthesized planar five-bar mechanism for chosen $\mathbf{a_1}$, $\mathbf{c_1}$

	p		q		r	
	δ_{px}	δ_{py}	δ_{qx}	δ_{qy}	δ_{rx}	δ_{ry}
Pose 1	0	0	0	0	0	0
Pos 2	0.022	0.0183	0.0279	0.0332	0.0192	0.0288
Pose 3	0.0297	0.0428	0.0439	0.0773	0.0235	0.0674
Pose 4	0.0354	0.0598	0.0555	0.1044	0.0281	0.0921

TABLE 8. Rigid-body pose tolerances achieved by for chosen $\mathbf{a_1}$, $\mathbf{c_1}$

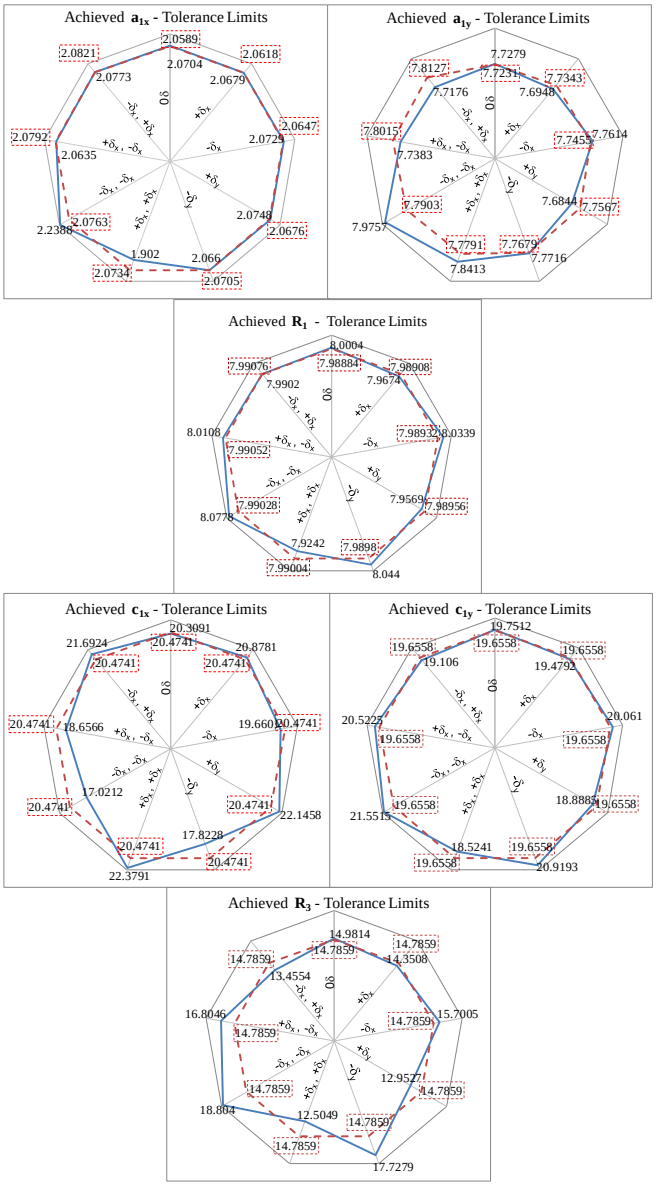

Fig. 6. Plots of synthesized moving pivot points with tolerance limits, dotted line denotes the best fit curve for the achieved moving pivots pose

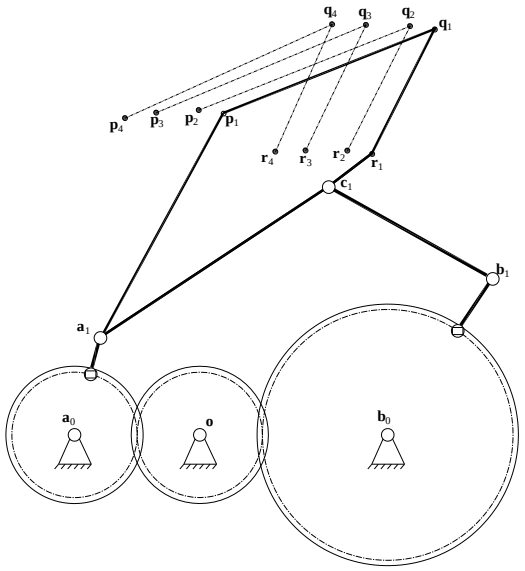

Fig. 7: Plots of synthesized motion generator

5. Discussion

When the pivots $\mathbf{a}_1$, $\mathbf{b}_1$, and $\mathbf{c}_1$ are collinear, the five-bar mechanism reaches a "lock-up" or binding position. The specific geared five-bar mechanism design considered in this work is one where $\mathbf{a}_0$-$\mathbf{a}_1$ is a link attached to the gear centered at $\mathbf{a}_0$ and $\mathbf{b}_1$ is a moving pivot on the gear centered at $\mathbf{b}_0$. Different types of gear-to-link attachments can be achieved. For example, the moving pivot $\mathbf{a}_1$ can be mounted directly to the gear centered at $\mathbf{a}_0$. Tooth alignment tolerance was not considered in the total gear train tolerance; since it would produce 3D effect on the coupler poses which is beyond the scope of this paper. The mathematical analysis software MathCAD was used to codify and solve the formulated motion with tolerance program.

6. Conclusions

Geared five-bar motion generation is used to synthesize a mechanism which passes through or approximates prescribed rigid-body positions. This work discussed the motion generation of geared five-bar mechanism with poses tolerance which is due to gear fabrication. ANSI/AGMA standards for gear fabrication tolerances were incorporated in the rigid-body poses displacement matrix. The synthesized mechanism approximate the prescribed rigid-body positions within the calculated gear train tolerances. Gear train tolerances presented herein are for spur gear type, similar tolerance analysis can be done for other gear types.

References

[1] C. H. Suh and C. W. Radcliffe, "Kinematics and Mechanism Design," John Wiley and Sons, New York, (1978).

[2] G.N. Sandor and A.G.Erdman, "Advanced Mechanism Design Analysis and Synthesis," Prentice-Hall, Englewood Cliffs, (1984).

[3] K. Lakshminarayana and G. Narayanamurthi, " On the Analysis of the Effect of Tolerances in Linkages," Journal of Mechanisms, Vol. 6, pp. 59-67 (1971).

[4] R.S. Hartenberg and J. Denavit, "Kinematic Syntheses of Linkages," McGraw-Hill, New York (1964).

[5] M.J. Tsai and T.H. Lai, "Accuracy analysis of a multi-loop linkage with joint clearance," Mechanism and Machine Theory, Vol. 43, pp. 1141-1157 (2008).

[6] M.J. Tsai and T.H. Lai, "Kinematic Sensitivity analysis of linkage with joint clearance on transmission quality," Mechanism and Machine Theory, Vol. 39, pp. 1189-1206 (2004).

[7] K.L. Ting, J. Zhu and D. Watkins, "The effect of joint clearance on position and orientation deviation of linkages and manipulators," Mechanism and Machine Theory, Vol. 35, pp. 391-401 (2000).

[8] V. Parlaktaş, E. Söylemez and E. Tanik, "On the synthesis of a geared four-bar mechanisms," Mechanism and Machine Theory, Vol. 45, pp. 1142-1152 (2010).

[9] S.Erkaya and I. Uzmay, "Determining link parameters using genetic algorithm in mechanisms with joint clearance," Mechanism and Machine Theory, Vol. 44, pp. 222–234 (2009).

[10] M.A. Laribi, A. Mlika, L. Romdhane, S. Zeghloul, "A combined genetic algorithm–fuzzy logic method (GA–FL) in mechanisms synthesis," Mechanism and Machine Theory, Vol. 39, pp. 717–735(2004).

[11] N. Diab, A. Smaili, "Optimum exact/approximate point synthesis of planar mechanisms," Mechanism and Machine Theory Vol. 43, pp. 1610–1624 (2008).

[12] Y.M. Al-Smadi, K. Russell and R.S. Sodhi, "Geared Five-Bar Path Generation with Structural Constraints," CSME, Vol. 17(8), pp. 1059-1072 (2009).

[13] ANSI/AGMA 2000-A88 Standards, "Gear Classification and Inspection Handbook," March 1988

[14] S.A. Kolhatkar and K.S. Yajnik, "The Effect of Play in the Joints of a Function-Generating Mechanism," Journal of Mechanisms, Vol. 5, pp. 521-532 (1970).

[15] R.E. Garrett and A. S. Hall, "Effect of Tolerance and Clearance in Linkage Design," ASME Journal of Engineering for Industry, pp.198-202, (1969).

[16] B.M. Imani and M. Pour "Tolerance analysis of flexible kinematic mechanism using DLM method," Mechanism and Machine Theory, Vol. 44, pp. 445-456 (2009).

[17] J.W. Wittwer, K.W. Chase and L.L. Howell, "The direct linearization method applied to position error in kinematic linkages," Mechanism and Machine Theory, Vol. 39, pp. 681-693 (2004).

[18] C.T. Brown, "Statistical models for position and profile variation in mechanical assemblies," M.S. Thesis, Brigham Young University, Provo, Utah, 1995.

[19] Z. Shi, "Synthesis of Mechanical Error in Spatial Linkages Based on Reliability Concept," Mechanism and Machine Theory, Vol. 32, No. 2, pp. 255-259 (1997).

[20] K. Russell and R.S. Sodhi, "Kinematic Synthesis of RRSS mechanisms for multi-phase motion generation with tolerances," Mechanism and Machine Theory, Vol. 37, pp. 279-294 (2002)

[21] M.H. Mousa, K. Russell and R.S. Sodhi, "Multi-Phase Motion Generation Of Five-Bar Mechanisms With Prescribed Rigid-Body Tolerances," Transaction of CSME, Vol. 30, Issue 4, pp. 459-472 (2006).

[22] S. Caro, F. Bennis and P. Wenger, "Tolerance Synthesis of Mechanisms: A Robust Design Approach," ASME Journal of Mechanical Design, Vol. 127, pp. 86-94 (2005).